

Adsorption and the Chemical Reaction $\text{N}_2\text{O}_4 \leftrightarrow 2\text{NO}_2$ in the Presence of N_2 in a Gas Phase Connected with a Carbon Nanotube

Somphob Thompho, Siegfried Fritzsche, Tatiya Chokbunpiam, Tawun Remsungnen, Wolfhard Janke, and Supot Hannongbua*



Cite This: *ACS Omega* 2021, 6, 17342–17352



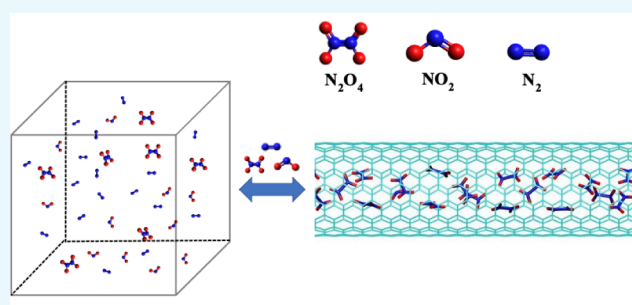
Read Online

ACCESS |

Metrics & More

Article Recommendations

ABSTRACT: The paper shows, by molecular simulations, that a CNT (9,9) carbon nanotube allows very efficient separation of nitrogen oxides (NO_x) from N_2 , that has in good approximation properties of the complete air mixture. Gibbs ensemble Monte Carlo simulations are used to describe the adsorption. The permanent chemical reaction between N_2O_4 and NO_2 , which occurs simultaneously to adsorption, is treated by the reactive Monte Carlo simulation. A very high selectivity has been found. For a low pressure and at $T = 298$ K, an adsorption/reaction selectivity between NO_x and N_2 can reach values up to 3×10^3 .



INTRODUCTION

Due to its severe threat to human health, air pollution has become a serious environmental problem especially in developing countries and also in highly industrialized countries. Besides fine dust particulate matter ($\text{PM}_{2.5}$), also gases like sulfur dioxide (SO_2) and nitrogen oxides (NO_x) play an important role.¹ NO_x can be produced by lightning, volcanos, and other natural sources, but main sources are human activities like combustion engines.

To protect the environment, significant efforts have been made in designing systems to eliminate NO_x emissions from fossil fuel combustion or from air. Common methods to remove NO_x are selective catalytic reduction² or the storage as nitrates. Another way is to use porous materials like activated carbon, zeolites, and metal–organic frameworks (MOFs) for the separation of NO_x from other gases by selective adsorption. It seems promising to investigate how the use of such materials can save energy and expensive equipment in comparison to other methods. To make such decisions, detailed knowledge about the basic mechanisms of the adsorption of NO_x in porous materials can be very helpful.

In air, NO_x are present mainly as NO_2 and N_2O_4 . NO , if present together with oxygen, will mainly be oxidized to NO_2 . NO_2 and N_2O_4 are in a permanent chemical reaction with each other



The equilibrium state of this reaction strongly depends upon the temperature and also upon the pressure. Chao et al.³ investigated this reaction in experiments. At room temperature and at lower temperatures, most of the NO_x molecules are

N_2O_4 , while at higher temperatures, most of the NO_x molecules are NO_2 . Hence, investigation of the separation of NO_x from air must take into account this reaction except at very high and at very low temperatures where only NO_2 or only N_2O_4 exist. An example is the paper of Chokbunpiam et al. where the separation of NO_2 from air at 374 K using several Zeolitic Imidazolate Framework (ZIF) materials was investigated.⁴ It was sufficient to consider only NO_2 because at 374 K, the NO_x exist almost entirely as NO_2 . The chemical reaction is described and discussed in more detail in the Supporting Material of Fritzsche et al.⁵

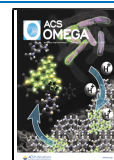
Adsorption of NO_x on porous materials for separation purposes has been examined in several papers,^{6–14} which are discussed in more detail in ref 5. Taking reaction 1 into account should improve the accuracy of the results.

The adsorption of NO_x by zeolite materials taking into account the chemical reaction (reaction 1) was examined in the pioneering paper of Matito-Martos et al.¹⁵ in the Grand Canonical Monte Carlo (GCMC) computer simulations and the reactive Monte Carlo (RxMC) simulations. However, in ref 15, only the NO_x without the presence of other gases have been considered. The interesting question of use of this type of adsorption and reaction for the separation of both NO_2 and N_2O_4 from air (or from N_2 , respectively) under the

Received: March 17, 2021

Accepted: June 16, 2021

Published: June 29, 2021



consideration of the chemical reaction (reaction 1) has only been investigated in ref 5. Fritzsche et al.⁵ used the Gibbs ensemble Monte Carlo (GEMC) and RxMC simulations to investigate the adsorption and reaction of a ternary mixture, $N_2O_4/NO_2/N_2$, on the MOF material MIL-127. To characterize the selectivity between the total amount of NO_x and that of N_2 , the ratio of N atoms in all NO_x molecules ($N_2O_4 + NO_2$) to N atoms in N_2 in the gas phase, or in the adsorbed phase, respectively, has been used in ref 5 to treat the ternary mixture like a binary mixture. We will also do that in the present paper for two reasons. The total number of N atoms in NO_x ($N_2O_4 + NO_2$) is not affected by the chemical reaction (reaction 1). Moreover, the common formula for the selectivity of a binary mixture¹⁶ can thus be used for the ternary mixture as well in the following way. Selectivity S_{ar} was defined in ref 5 by the following equation:

$$S_{ar} = \frac{N_{NO_x,B} N_{N_2,A}}{N_{N_2,B} N_{NO_x,A}} \quad (2)$$

where S_{ar} is the selectivity due to both adsorption and reaction; $N_{NO_x,A}$ and $N_{NO_x,B}$ are the sum of the numbers of all N atoms contained in all NO_x in the gas phase (box A) or in the adsorbed phase (box B) of the Gibbs ensemble, respectively; and $N_{N_2,A}$ and $N_{N_2,B}$ are the number of N atoms in N_2 in box A and box b, respectively.

In the work of Fritzsche et al.,⁵ the NO_x/N_2 selectivity, defined by formula 2, for MIL-127, was found to be up to almost 1000 at 298 K and 2 bar for a concentration of NO_x that was characterized by the ratio 1:40 of N atoms in NO_x ($N_2O_4 + NO_2$) to N atoms in N_2 in the gas phase. For a higher concentration of NO_x and for a higher temperature, the selectivity was smaller. Lower concentrations of NO_x have not been considered because the number of NO_x molecules would then be too small for a reasonable statistics in the simulations. The air was represented by N_2 in the work of Fritzsche et al.⁵ because N_2 not only forms the main part of air, but tests and earlier work show also that the adsorption behavior of O_2 on several porous materials was found to be very similar to that of N_2 .^{4,17}

For the work of Fritzsche et al.⁵ the metal–organic framework MIL-127 has been chosen to investigate the strong separation effect because the pores and channels of this material are only slightly larger than the size of the N_2O_4 molecule. Hence, strong van der Waals forces could be expected. However, the question remained open whether other materials can show even higher, may be even much higher, performance. The very high separation performance, which was found in the paper by Kowalczyk,¹⁸ by CNTs for the H_2/CO_2 separation prompted us to ask whether such a performance can also be reached using a CNT for the ternary system NO_x/N_2 . It was also interesting to find out if the cations, which are present in zeolites discussed in the work of Matito-Martos et al.¹⁵ and the MOFs discussed in the work of Chokbunpiam et al. and Fritzsche et al.,^{4,5} but not in the CNT model employed in our present simulations, play a role in the extraordinarily high selectivity.

A test and comparison of many materials for this purpose in one study was not possible because the simultaneous simulation of reaction and adsorption under the condition of constant pressure and at constant concentrations of the molecule sorts in the gas phase is difficult and computer-time expensive.

In the work of Fritzsche et al.,⁵ it turned out that the very large negative potential energy of the N_2O_4 molecules within the channels and cavities of MIL-127 was decisive for the high selectivity. This potential energy is caused by the attraction of N_2O_4 from the lattice, which is stronger in smaller channels and cavities because of the vicinity of many lattice atoms in different directions at the same time. Therefore, we have chosen a narrow CNT (9,9) for this investigation. Cations are missing in the CNT model that we use.

Additional molecular dynamics (MD) simulations have been carried out in order to be sure that in such a narrow tube, all kinds of guest molecules can move.

CNTs have been synthesized first by Iijima and Ichihashi¹⁹ and Bethune et al.²⁰ in 1993. CNTs are large cylindrical molecules formed by a hexagonal arrangement of hybridized carbon atoms.²¹ They possess unique physical, electrical, chemical, and mechanical properties, and they are therefore one of the latest and promising materials for molecular mechanics and nanoelectronic devices. Their potential applications in a number of nanotechnologies have drawn intense interest since their discovery. De Volder et al.²² give an overview over such applications. For the development of single- and multiwalled carbon nanotubes, current methods include aerosol synthesis of carbon nanotubes, arc discharge, laser ablation, and catalytic/decomposition.²³

There are already some applications of CNTs as adsorbents. Kowalczyk¹⁸ reports the adsorption of several gases (CO_2 , CO , N_2 , H_2 , O_2 , and CH_4) on a double-walled CNT at 300 K. The GCMC simulations were used to examine the adsorption of pure gases, and mixture properties have then been calculated by ideal adsorbed solution theory (IAST). The adsorption selectivity computed by IAST reaches very high values for vanishing pressure, for example, up to 10^6 for CO_2/H_2 separation. In experiments, Feng et al.²⁴ used combined filters from MOFs and CNTs for efficient ultrafine dust removal and acid gas adsorption. They reported about the removal of SO_2 and NO_2 from a gas stream and their membrane, and that the experiment was very successful. They did not mention about N_2O_4 although under ambient conditions, a large part of NO_x will exist as N_2O_4 , even for the low partial pressure of NO_x .

Pandey et al.²⁵ showed that a CNT membrane was a successful candidate for the removal of toxic compounds from cigarette smoke. The authors used CNT filters with outstanding success in extracting PM2.5, with a removal efficiency of approximately 99%.

Such a high efficiency of CNTs for separation purposes led us to investigate, in the present paper, their use for the removal of NO_x from air. In this simulation paper, we focus on the details and interrelations of the involved effects. Similar to the work of Fritzsche et al.⁵ for MIL-127, we wanted to find out the influence of the chemical reaction (reaction 1) between NO_x on the separation process.

■ TECHNICAL DETAILS

Figure 1 illustrates the structure of a single-walled CNT (9,9) carbon nanotube. The tube consists of identical flat rings, where two adjacent ones are always rotated against each other around the common central axis. By shifting the double rings by $n \times 2.4595 \text{ \AA}$, where $n = 1,2,3,\dots$ along this common axis, the whole CNT (9,9) can be created. For our simulations, the structure of the CNT was generated by the Web-Accessible Nanotube Structure Generator.²⁶ A CIF file has been produced by the Avogadro software,²⁷ and the crystal has been optimized



Figure 1. Structure of the CNT (9,9) carbon nanotube. Left: Flat single ring formed by 18 carbon atoms. Middle: Double ring formed by two flat single rings. Right: Carbon nanotube consisting of 10 double rings.

using the CASTEP module implemented in Material Studio 5.5.²⁸ The optimization by the CASTEP software was done by BFGS optimization.²⁹ It was performed with the PBEPBE/6-31G(d) basis set in the MS studio program. The accuracy and power of this method have been validated by Milman et al.³⁰ for more than 180 parameters of numerous crystal types.

There are different potential parameter sets proposed for the graphene/CNT lattice. Zhang et al.³¹ examined the adsorption and selectivity of CH₄/CO₂ in functional-group-rich organic shales using GCMC simulations. These materials have in the wall the same hexagonal carbon network like the CNT lattice. They used Lennard–Jones (LJ) parameters, $\sigma = 3.47 \text{ \AA}$, $\epsilon/k_B = 47.9 \text{ K}$, for the carbon atom of the lattice, which indicates $\epsilon = 0.398 \text{ kJ/mol}$. The lattice was considered to be rigid and uncharged.

In the paper³² Pramanik et al. investigated CNTs that were dispersed in solvents and polymer solutions. They used a charged model for the CNT wall including π electrons for the interaction of the CNTs with the solution outside of the CNT. For the carbon atom these authors use the Lennard–Jones parameters $\sigma = 3.79 \text{ \AA}$, $\epsilon = 0.063 \text{ kcal/mol}$, that means $\epsilon = 0.264 \text{ kJ/mol}$. For the charge, they use $0.2e$ for the carbon kernel and $-0.1e$ for the π electrons. A flexible lattice was used.

For this work, the LJ parameters of the carbon have been taken from Kaukonen et al.³³ In ref 33, LJ parameters for the interaction of water with CNTs are developed by density functional calculations and compared with the literature. The parameters for the C atom are given in Table 1 together with the mass of the carbon atom. The lattice was considered to be rigid and uncharged.

Table 1. Averaged Lennard–Jones Parameters of the Carbon Atom in the Lattice of the CNT

	σ (Å)	ϵ (kJ/mol)	mass (g/mol)
C in CNT (9,9)	3.5340	0.2906	12.0

The LJ parameters, masses, and partial charges for the atoms within the guest molecules are given in Table 2. The parameters for NO_x have been taken from the paper of Bourasseau et al.³⁴ They have been used already in the two adsorption/reaction papers for NO₂/N₂O₄ [5,15]. The parameters for N₂ correspond to the TraPPE forcefield.³⁵ All these parameters for the guest molecules are the same that have been used already in the work of Fritzsche et al.⁵

The equilibrium constants for reaction 1 have been taken from the paper of Chao et al.,³ and a table is given in ref 36. The same source for the equilibrium constants has been used in refs 4 and 5. In the work of Matito-Martos et al.,¹⁵ this choice was confirmed by own calculations using the molecular partition functions of the molecules. The values of the

Table 2. Lennard–Jones Parameters, Masses, and Partial Charges of the Atoms of the Guest Molecules^a

	σ (Å)	ϵ (kJ/mol)	mass (g/mol)	charge (e)
N (in N ₂)	3.310	0.2993	14.01	-0.482
X (in N ₂)	0.0	0.0	0.0	0.964
N (in NO ₂)	3.240	0.4174	14.01	0.146
O (in NO ₂)	2.930	0.5179	16.01	-0.073
N (in N ₂ O ₄)	3.240	0.4174	14.01	0.588
O (in N ₂ O ₄)	2.930	0.5179	16.01	-0.294

^aX means a fictive charge center at the center of mass in N₂.

equilibrium constants in the paper³ have been measured at 1 atmosphere for the ideal gas and without geometrical restrictions by walls. The formula for the acceptance probability of a reactive move of the RxMC simulation at a given temperature and configuration of the system is based on the ideal gas equilibrium constant for this temperature and the potential energy of the involved molecules. This potential energy term will take into account the mutual interactions of the molecules in nonideal gases, and it will also yield the influence of the walls of cavities and channels.

In a restricted geometry, the degrees of freedom of rotation of the large N₂O₄ molecule will be reduced. This can reduce the equilibrium constant, and it can be taken into account formally by a reduction factor.^{37,38} For the CNT, such a factor can hardly be calculated, and it can also not be measured. Therefore, like in many papers,^{4,15} we use the ideal gas equilibrium constant as an approximation for the equilibrium constant at high dilution within restricted geometry. The question, if this reduction of the equilibrium constant can reduce the high selectivity, is answered in the Results and Discussion section, when we examine the influence of the reaction on the selectivity.

The investigations have been carried out at two temperatures, namely, 298 and 374 K. At lower temperatures, condensation could occur, which could not be handled by the simulation methods applied here. Higher temperatures would lead to reduced adsorption and selectivity, as derived in ref 17. A temperature of 374 K has been chosen for the higher temperature because the equilibrium constant for this temperature is given in ref 39.

For the pressure calculations by the Peng–Robinson equation (needed only for the presentation of the results), we only found the parameters given in ref 39 where identical parameters are given for both NO₂ and N₂O₄, which have been fitted from thermodynamic experiments for their mixture. Therefore, it would also be difficult to perform GCMC simulations based on chemical potentials for NO₂ and N₂O₄ from the Peng–Robinson equation. We have neglected the corrections with respect to cross correlations for mixtures of different sorts in the Peng–Robinson equation because these corrections would only slightly modify the deviations from ideal gas behavior, which themselves are quite small in our systems and we could not find cross correlation parameters for mixtures including NO_x in the literature. The corresponding parameters for N₂ have already been used in the work of Fritzsche et al.⁵

The interaction parameters used in the MD simulations are the same as in the GEMC simulations. For the rigid guest molecules, the trajectories have been calculated in the simulation software package DL_POLY by the SHAKE algorithm. The Coulomb potential of the partial charges of

the molecules was calculated by Ewald summation. The simulations have been carried out at 298 K for the first 256 Å of the tube length with guest molecules at 298 K and 0.5 bar. The percentage of N atoms in NO_x was 10% of all N atoms in the gas phase of the corresponding GEMC simulation. The particle numbers and their initial positions have been taken from a snapshot of this GEMC simulation. Thus, the number of N_2O_4 molecules within the short part of the CNT, which was considered in the MD, was 108. The number of NO_2 molecules within this part of the tube is only 5 and the number of N_2 molecules would have been 0 in the snapshot. To check their mobility, two N_2 molecules have been added to the snapshot of this part of the tube at random positions. This is realistic because in the complete CNT of the GEMC simulations, there are two N_2 molecules and they could in principle just be found in this part of the tube as well.

During the simulations, the frequency ratio of Monte Carlo moves for translation, rotation, swap to the other box, and the reactive move is 10:10:2:1.

Under real conditions, the concentration of NO_x in the air is too small to allow a reasonable statistics if the total number of particles in the simulation is not extremely large. Therefore, we examined higher concentrations. However, to be as close to reality as possible, the NO_x concentration should be small enough that the NO_x molecules rarely meet each other. To get an impression about the influence of the concentration, we considered two different concentrations (5 and 10%). The computational effort of these simulations is quite high. Therefore, it would not have made much sense to investigate many concentrations, which all are above the concentrations found in nature.

The numbers of molecules in the gas phase during the GEMC simulations vary from run to run. Typically, there are about 2500 N_2 molecules in the gas box. The ratio of the molecule numbers of N_2O_4 and NO_2 depends upon the pressure and temperature because of chemical reaction (reaction 1). For example, in a snapshot at 298 K and 10 bar, there are 2762 N_2 molecules, 244 N_2O_4 molecules, and 95 NO_2 molecules in the final equilibrium state in the gas phase. They are in equilibrium with 1038 N_2O_4 molecules, 208 NO_2 molecules, and 44 N_2 molecules that are adsorbed on the CNT.

The CNT have a stability against mechanical stress that is higher than that of steel. This property is being used in numerous applications. Therefore, we neglected possible small deformations of the CNT by adsorbents. The temperature should be below the temperature at which coal starts to burn since all CNTs consist of pure carbon.

Like in most theoretical studies, simplifications make the treatment feasible. We have neglected the influences from outside of the tube, the elasticity of molecules and tube, and the presence of other substances. These additional perturbations are out of the range of this study. Mixtures of more than two species are rare in the literature. We investigated a ternary mixture with a quite high computational effort. To include additional effects would be an interesting subject for further studies that require very high computational resources.

A piece of about 250 nm length of a single nanotube is considered. To avoid boundary effects, periodic boundary conditions have been applied in the axis direction; therefore, the tube is quasi-infinite in the axis direction. The material that could be surrounding the tube, like other tubes, air, or another material, was not taken into account. This seems to be justified

because the effect under consideration is due to the interaction of, for example, a single N_2O_4 molecule with many wall atoms that are close to it because of the small tube diameter. This will be examined in detail in the Results and Discussion section. The influence of other (also attractive) LJ force centers outside the tube at a larger distance than the wall atoms should not reduce the strong attraction by the wall considerably.

RESULTS AND DISCUSSION

Pure Substances (Fictitious Systems). In the work of Fritzsche et al.,⁵ it turned out that the reason of the very high selectivity was the strong adsorption of N_2O_4 because of its very low potential energy within MIL-127. Hence, we checked first if such low potential energies of N_2O_4 appear also in the CNT. It was found in refs 5 and 15 that, within the restricted space of nanopores, NO_x exist mainly as N_2O_4 . However, the gas phase containing only NO_2 or only N_2O_4 is fictitious, and it is simulated here only to collect additional knowledge about the system.

First, we carried out potential energy calculations for different positions and orientations of a single N_2O_4 molecule within the CNT, as illustrated in Figure 2.

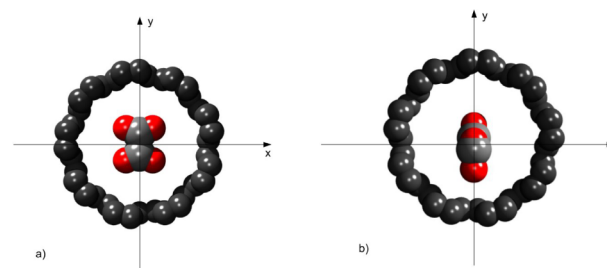


Figure 2. Two orientations of the N_2O_4 molecule within the tube. Orientation (a) shows the flat N_2O_4 molecule in the xy -plane perpendicular to the z -axis. Orientation (b) shows the N_2O_4 molecule in the yz -plane perpendicular to the x -axis.

Figure 3 shows the potential energy for a single N_2O_4 molecule at different positions with the center of mass (COM) on the x -axis if the molecule in orientation (a) or (b) is moved along the x -axis. The potential energy values are very low, particularly if the molecule orientation is parallel to the wall at a distance of the COM of 2.3 Å from the wall, i.e., if the flat molecule is directly lying on the wall of the CNT. The

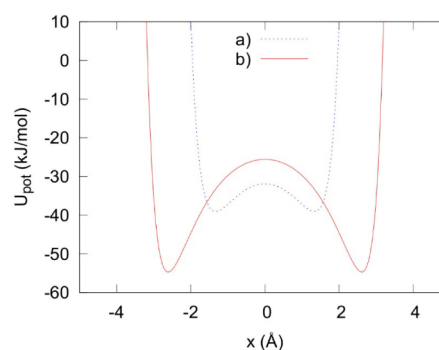


Figure 3. Potential values that result if the molecule in orientation (a) or (b) (as defined in Figure 2) is moved along the x -axis. The x coordinates in Figure 3 are the x coordinates of the center of mass of the N_2O_4 molecule.

potential energy of the molecule in this configuration is -54.7 kJ/mol. This indicates that a molecule trapped there would need this amount of kinetic energy to escape to the gas phase. Compared with the average kinetic energy of translation $3/2 \times k_B T = 2.48$ kJ/mol of the molecule at 298 K, this is a very low potential energy.

We also examined the adsorption of pure N_2 , N_2O_4 , and NO_2 even though N_2O_4 and NO_2 without chemical reaction (reaction 1) between them will not exist in nature under ambient conditions. These data should only help to understand the adsorption behavior of the species. The results can be compared with those of realistic mixture simulations to learn how dominating the N_2O_4 adsorption is for the whole process.

Figure 4 shows the amount of pure N_2O_4 , NO_2 , and N_2 that would be adsorbed in the CNT as a function of pressure if

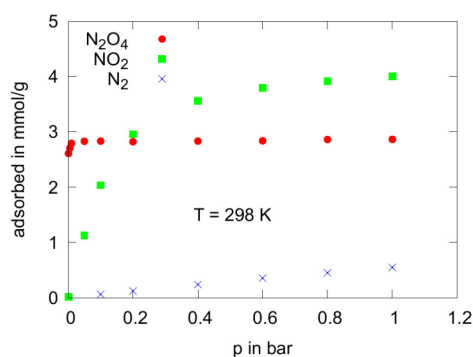


Figure 4. Adsorption isotherm for the adsorption of pure N_2O_4 , NO_2 , and N_2 at 298 K if the pure N_2O_4 or NO_2 would exist.

these systems would exist. Pure N_2 , of course, exists. For the artificial systems, it turned out that the saturation of pure N_2O_4 is reached already at a very low pressure of about 0.05 bar. This is due to the low potential energy of the N_2O_4 molecules within the CNT, which is demonstrated in Figure 3. The average potential energy per N_2O_4 molecule found in this simulation at 298 K and 1 bar is about -57.3 kJ/mol. This value is even lower than the minimum in Figure 3. The difference is obviously due to the mutual interaction of the N_2O_4 molecules. These very low potential energy values indicate that in this simulation, the flat N_2O_4 molecules must have orientation (b) and they must be situated close to the CNT wall, i.e., on the inner surface of the tube. The adsorption of pure NO_2 also increases with pressure faster than that of pure N_2 in this fictitious system. For pure NO_2 at 298 K, the

average potential energy is -28.0 kJ/mol. Note that the potential energy enters the canonical partition function in the exponent, and a small difference in the potential energy can enhance the probability of a state considerably.

It is known that in the real system, spatial restrictions favor the concentration of N_2O_4 molecules in comparison with NO_2 molecules by the chemical reaction (reaction 1).^{5,15} Hence, the adsorbed NO_x will exist mainly in the form of N_2O_4 molecules. Therefore, particularly for the very low pressure, a very high NO_x/N_2 selectivity at 298 K can be expected, considering the information in Figure 4. Interestingly, the adsorbed amount of pure NO_2 in Figure 4 is higher than that of N_2O_4 . It is measured in mmol/g, as shown in Figure 4. This indicates that essentially the numbers of molecules are compared. Since one N_2O_4 molecule is composed of two NO_2 molecules, the adsorbed mass of almost 3 mmol/g of N_2O_4 in Figure 4 corresponds to a mass of NO_x that is equal to the mass of almost 6 mmol/g of NO_2 . Moreover, in the mixture that corresponds to a realistic system, the N_2O_4 molecules will occupy the strongest adsorption sites. Therefore, it is to be expected that less NO_2 molecules than indicated in Figure 4 would be adsorbed in the realistic system and, moreover, the recombination reaction will convert most of them into N_2O_4 .

MIXTURES (REALISTIC SYSTEMS)

Figure 5 shows the adsorbed amounts of the different species at 374 K for the system in which the N atoms in NO_x molecules make up 5 or 10% of all N atoms within the gas phase (simulation box A). The number of N atoms in NO_x molecules in the adsorbed phases is clearly much larger than 5 or 10% of all N in all guest molecules, which indicates high NO_x/N_2 selectivity. This selectivity can be seen in Figure 6. In agreement with the same adsorption/reaction process in MIL-127⁵ at 374 K, the selectivity increases with increasing pressure. A possible reason is that the percentage of N_2O_4 among NO_x is increasing with increasing pressure, as can be seen in Figure 7.

In Figure 7, the ratio of molecule numbers $N_2O_4/(N_2O_4 + NO_2)$ at 374 K as a function of the pressure in box A and box B can be seen. As mentioned in Introduction, at this high temperature in the gas phase at ambient pressure, NO_x exist almost exclusively as NO_2 . Within the CNT, the restricted space leads to the existence of some more N_2O_4 molecules particularly at a higher pressure. As expected, the ratio is increasing with increasing pressure, and at the given pressure, it is higher in box B than in box A. All these findings are in

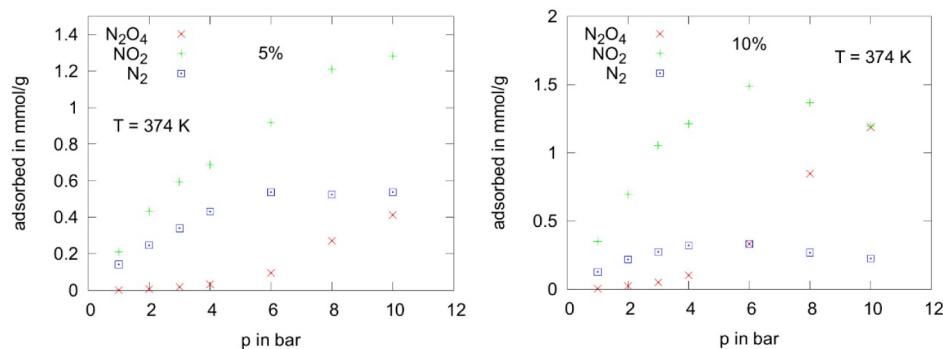


Figure 5. Amount of adsorbed gases in the CNT at 374 K. Left: The number of N atoms in NO_x molecules is 5% of the number of all N atoms within the gas phase. Right: The number of N atoms in NO_x molecules is 10% of the number of all N atoms within the gas phase.

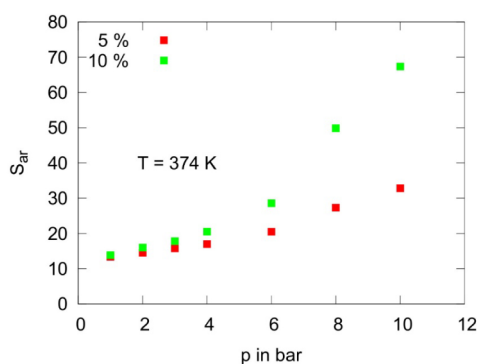


Figure 6. Selectivity S_{ar} of NO_x with respect to N_2 for the ternary mixture, as defined in eq 2.

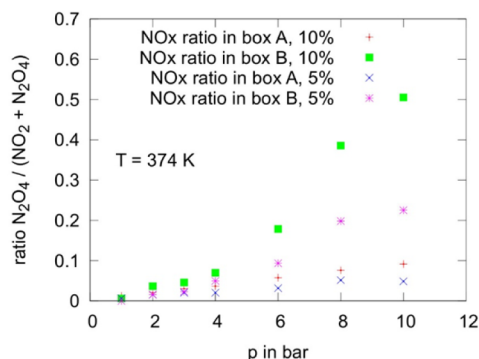


Figure 7. Ratio of the number of N_2O_4 molecules to that of all NO_x molecules ($\text{N}_2\text{O}_4 + \text{NO}_2$) at 374 K as a function of the pressure in box A and box B for percentages of N atoms in NO_x to all N atoms in the gas phase of 10 and 5%, respectively.

agreement with Le Chatelier's principle because the recombination reaction reduces the total number of particles. Interestingly, the ratio in box B (adsorbed phase) at a given pressure is significantly higher for a higher percentage of NO_x in the ternary mixture in the gas phase. This is also to be expected because the partial pressure of NO_x is higher at a higher concentration.

During the simulations for $T = 298$ K, it turned out that a very small amount of N_2 is adsorbed in box B (the CNT). This is no problem for adsorption isotherms but this is a problem for the selectivity. According to eq 2, the calculation of the selectivity requires division by the number of adsorbed N_2 molecules. If this number is orders of magnitude smaller than

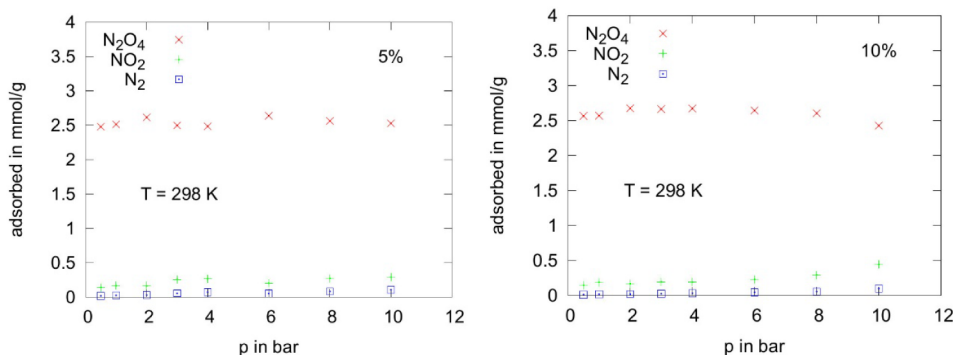


Figure 8. Amount of adsorbed gases in the CNT at 298 K. Left: The number of N atoms in NO_x molecules is 5% of the number of all N atoms within the gas phase. Right: The number of N atoms in NO_x molecules is 10% of the number of all N atoms within the gas phase.

the number of adsorbed NO_x , then each small change in the number of adsorbed N_2 leads to a large change in the selectivity. It is a division by a number close to zero. Therefore, after equilibration, we carried out 8 runs of 100 million of steps and averaged each result over these 8 runs to improve the accuracy.

Figure 8 shows the adsorbed amounts of the different guest molecule sorts in the mixture at 298 K. Interestingly, the amount of adsorbed N_2O_4 is almost the same for both concentrations and at all pressures. This indicates that saturation with N_2O_4 is reached at a very low pressure even for the lower concentration. Thus, a very high selectivity is to be expected.

This selectivity, defined in eq 2, can be seen in Figure 9. The high selectivity at a low pressure can be compared with the

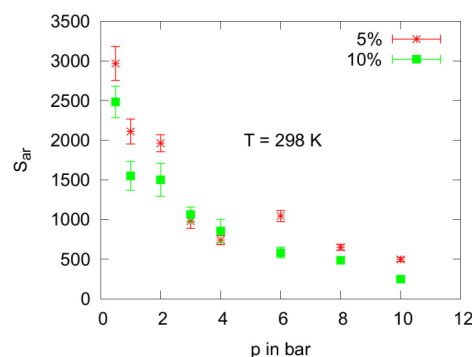


Figure 9. Selectivity S_{ar} of NO_x with respect to N_2 for the ternary mixture, as defined in eq 2, as a function of the pressure at 298 K.

similar high selectivity that was found at a low pressure by Kowalczyk for CO_2/H_2 separation with CNTs.¹⁸ They found even 2 orders of magnitude higher selectivities up to 10^6 . Small changes in the very low number of adsorbed N_2 molecules cause huge fluctuations in the selectivity, as explained above. Even after averaging over 8 runs of 100 million of steps, Figure 9 shows large scattering of the values. Eight results are not enough to form a reasonable Gaussian distribution. Therefore, we have shown in Figure 8 by error bars the uncertainty, which is defined to be half of the difference between the largest and the smallest result for this data point among the eight values. We believe that the extremely large selectivity of about 2500–3000 at 1 bar can be seen clearly enough. The effort to reduce the fluctuations to 10% of the present value would be 100 times larger than the effort that we put. We believe that such

an effort is not worthwhile. We believe that the main result, namely, the selectivity that exceeds 1000 by far, can be seen from the present curve as well.

The dependence of the selectivity on the concentration of NO_x in the gas phase is quite small. The difference in the selectivity for 5 and 10% is smaller than the fluctuations.

Figure 10 shows the ratio of the number of N_2O_4 molecules to that of all NO_x molecules ($\text{N}_2\text{O}_4 + \text{NO}_2$) as a consequence

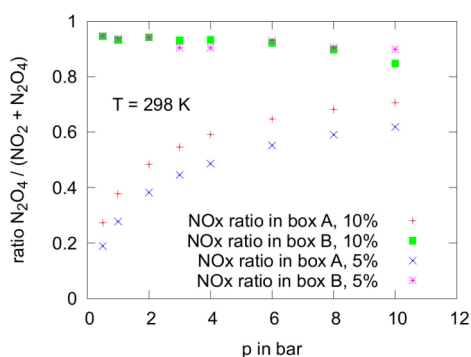


Figure 10. Ratio of the number of N_2O_4 molecules to that of all NO_x molecules ($\text{N}_2\text{O}_4 + \text{NO}_2$) at 298 K as a function of the pressure in box A and box B for percentages of N atoms in NO_x to all N atoms in the gas phase of 10 and 5%, respectively.

of reaction 1 in the gas phase and in the adsorbed phase at 298 K and at different pressures and concentrations. These results are in agreement with Le Chatelier's principle, as discussed above.

The high selectivity is connected with the strong adsorption of the N_2O_4 molecules within the CNT. Therefore, the spatial distribution of their positions within the CNT for such conditions under which the high selectivity appears deserves detailed examination.

Figure 11 shows a histogram of the distance of the centers of mass of the N_2O_4 molecules within the CNT from the central

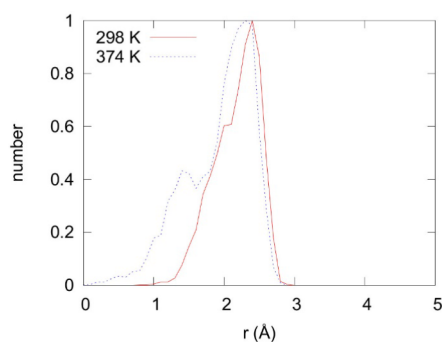


Figure 11. Distribution of the distances of the centers of mass of the N_2O_4 molecules within the CNT from the central axis at $p = 1$ bar and if 10% of all N atoms in the gas phase are those of NO_x . The curves are normalized by the division of the numbers by the maximum number for each curve separately.

axis. The distance from the central axis to the centers of the carbon atoms of the wall is about 6.1 Å. During an evaluation run of 1 million steps at $T = 298$ K, the positions of all of the approximately 1100 N_2O_4 molecules have been checked every 1000 steps. For $T = 374$ K, the same has been done in a longer evaluation of 10 million steps to compensate, to some extent, the smaller amount of N_2O_4 molecules within the tube.

The LJ diameter σ of the carbon atoms is 3.53 Å and that of the oxygen atoms is 2.93 Å. Therefore, as shown in Figure 11, the distance between the maximum of the distribution and the centers of the nearest lattice atoms is not much more than the sum of the radii of both atoms. This indicates that most of the N_2O_4 molecules have an orientation that corresponds to orientation (b) shown in Figure 2 and that they are situated close to the wall. Interestingly, the inflection in the histogram curve at about 2 Å for $T = 298$ K and at about 1.5 Å for 374 K is not caused by fluctuations because we could also find it by analyzing different shorter parts of the trajectory. It can be assumed that this indicates that some of the adsorbed molecules can be found in orientation (a) according to Figure 2.

In Figure 12, the radial density functions (RDFs) and the corresponding number integrals between the N atoms of different N_2O_4 molecules and between the N atoms of N_2O_4 with the C atoms in the wall of the tube can be seen. The guest–guest (gg) RDF shows a peak at about 4.1 Å that corresponds to an inflection in the corresponding number integral. It can be explained by a regular order of the N_2O_4 molecules with respect to each other. From Figure 11, it can be concluded that this must be a regular two-dimensional order along the tube wall. Note that for large distances, the RDF does not approach 1.0 like in a gas or liquid without geometrical restrictions. The reason is that the part of the tube that will be cut by a spherical shell of large radius will occupy only a very small part of the complete spherical shell. Hence, the number of particles encountered there divided by the volume of the complete shell (corresponding to the definition of the RDF) gives a particle density that is very small.

The large fluctuations in the gg RDF in Figure 11 for $T = 374$ K are caused by the small amount of N_2O_4 that are adsorbed in the CNT at this temperature and at $p = 1$ bar. The average particle density can be estimated. From Figure 11, it can be concluded that the centers of mass of the N_2O_4 molecules are essentially situated within distances up to 3 Å from the tube axis. The length of the tube is about 2460 Å. This indicates that a volume of about $7 \times 10^4 \text{ \AA}^3$ is accessible for the molecules. At $T = 374$ K and $p = 1$ bar on the gas phase, there are, on average, only about 2.7 N_2O_4 molecules adsorbed on the CNT, and the average particle density is therefore about $n = 4 \times 10^{-5} \text{ \AA}^{-3}$. Therefore, the number integral that gives the average number of neighbors within a given distance almost vanishes at $T = 374$ K, and the question about a shell of neighbors is irrelevant in this case and the number integral would be useless. Therefore, it is not shown in Figure 12.

To illustrate the structure of the adsorbed gas for an example case in which we found high selectivity, the tube with molecules has been shown in Figure 13. The configuration at 298 K and 0.5 bar has been chosen. The percentage of N atoms in NO_x was 10% of all N atoms in the gas phase. According to Figure 10, almost only N_2O_4 will be found inside the tube, and Figure 11 shows that their preferred position is close to the wall. However, there is also a portion of the N_2O_4 molecules that are moving closer to the middle of the tube. Figure 13 confirms this structure. None of the few NO_2 or N_2 molecules can be seen in these snapshots.

Test of the Importance of the Reaction for the Selectivity. In addition to the realistic adsorption and reaction simulations, such as that mentioned in the work of Fritzsche et al.,⁵ test simulations have been performed to see if

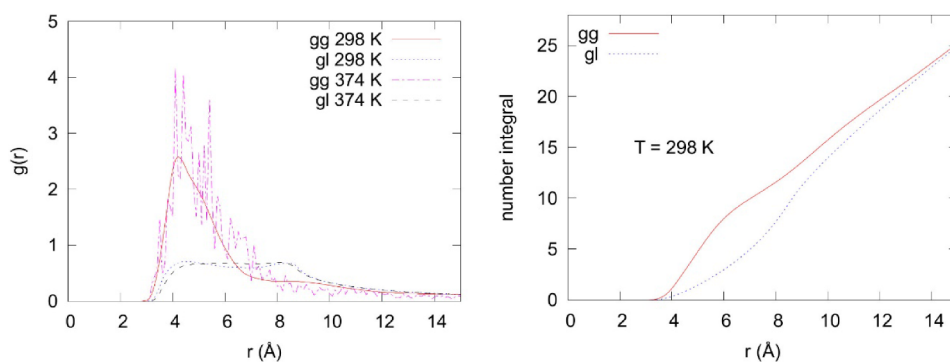


Figure 12. Left: RDF of a N atom in N_2O_4 with a N atom in another N_2O_4 molecule (gg means guest–guest) and of a N atom in N_2O_4 with the carbon atoms in the wall (gl means guest–lattice) at $T = 298$ K and 374 K at $p = 1$ bar. Right: The corresponding number integrals for 298 K.

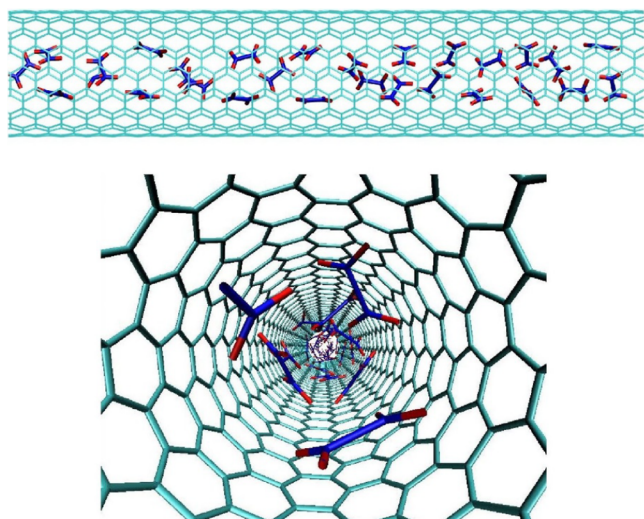


Figure 13. Guest molecules within the CNT. Top: A magnified part of the tube with N_2O_4 molecules. Both tube and N_2O_4 molecules as stick models where red means oxygen and blue means nitrogen. Bottom: View along the tube axis on some N_2O_4 molecules.

the high selectivity, which was found at 298 K and at low pressure, is caused mainly by the chemical reaction or mainly by the adsorption. We started from the final state of the simulation run at 1 bar, 298 K, with N atoms in NO_x being 10% of all N atoms in box A (gas phase) corresponding to the data point in the curves shown above. In the evaluation run of 100 million steps with reaction, the selectivity was found to be 1429. We then continued this run, but switched off the reactive MC moves. In order to have equal conditions in comparison with the reactive run the particle numbers in box A have been kept constant at the values that they had in the run with reaction. This has been done by adding or removing particles in order to keep the particle numbers in box A constant, whenever the adsorption has changed these numbers. The situation in box B was then the result of pure adsorption. We carried out 3 additional equilibration runs of 100 million steps without chemical reaction. Then, in an evaluation run of 100 million steps, also without the chemical reaction, the selectivity was found to be 1803. This indicates that the high selectivity is caused by selective adsorption and not by the reaction. Moreover, the selectivity is reduced somewhat by the chemical reaction. This is in agreement with the findings of Fritzsche et al.⁵ The question, whether small corrections in the rate

constant because of the restricted space would reduce the selectivity, is therefore meaningless.

MD Calculations of the Translational Behavior of the Guest Molecules. MD simulations have been carried out at 1 bar, with 10% of the N atoms in the gas phase being included in NO_x molecules. This is one of the configurations with high selectivity. The trajectories of all molecules of the three sorts are calculated starting from a snapshot of the GEMC simulation. The particle numbers adsorbed on the CNT are 108 N_2O_4 , 6 NO_2 , and 2 N_2 for this snapshot.

In good approximation, the chemical reaction can be neglected in this MD simulation because GEMC and RxMC simulations showed that mostly N_2O_4 molecules are present in this system.

From the trajectories, the mean-square displacement (MSD), here called $M(t)$, can be calculated for each sort of molecules. The MSD for N molecules of a given sort is defined by

$$M(t) = \frac{1}{N} \sum_{i=1}^N (\vec{r}_i(t) - \vec{r}_i(0))^2 \quad (3)$$

where $\vec{r}(t)$ is the position vector of the molecule number i of this sort at time t .

Figure 14 shows the mean-square displacements of the N atoms belonging to different molecules, as obtained from MD simulations as a function of time. Interestingly, in spite of the narrow tube, the time dependence of all three MSDs is that of normal diffusion. In particular, for the quite large N_2O_4 , it seemed to be possible that these molecules are too big to pass each other in the tube. Thus, single-file diffusion could be

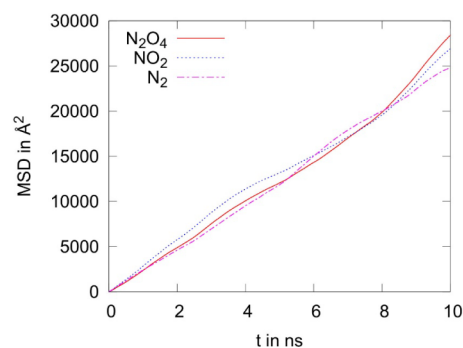


Figure 14. Mean-square displacements of the nitrogen atoms belonging to different molecules, as obtained from MD simulations.

possible (see the review article of Kärger).⁴⁰ The consequence of single file diffusion would be, that the MSD of N₂O₄ molecules would increase with time less than linearly. The question whether the N₂ molecules can escape from the tube can be clearly answered: They can move over large distances. This is confirmed by Figure 14. The square of the diameter of the region of the tube that is accessible for N₂ is less than 50 Å², while the MSD after 10 ns is more than 25 000 Å². This corresponds to average shifts of about 160 Å, which are only possible in the axis direction. Note, however, that the MSDs fluctuate around each other. Because of the very different sizes, shapes, and masses of the molecules, the diffusion behavior of the different species could be expected to be different. Thus, the agreement of the MSDs is a very clear indication of collective diffusion.

The self-diffusion coefficient D_s for one-dimensional diffusion can be calculated for large times t by

$$D_s = \frac{M(t)}{2t} \quad (4)$$

The self-diffusion coefficient of all three sorts of molecules is about 1.4×10^{-8} m²/s.

CONCLUSIONS

The separation of NO_x from air (which was represented by N₂) by selective adsorption was investigated by a combination of GEMC and RxMC simulations. The RxMC simulation was needed because under ambient conditions, NO₂ and N₂O₄ are in permanent dissociation/recombination equilibrium. Simulations have been performed in which the ratio of the sum of N atoms in NO_x in the ternary mixture N₂/NO₂/N₂O₄ in the gas phase was 10% of all N atoms in the gas phase, and also simulations in which this ratio was 5% have been performed. The number of N atoms within all NO_x, which is not changed by the chemical reaction, has been chosen to monitor the separation of NO_x from the mixture. It was found that CNTs are well suited to separate NO_x from air by selective adsorption. Extraordinary high selectivity has been observed at a low pressure. At 0.5 bar, 298 K, this selectivity could reach the value of 3×10^3 . This high selectivity at low pressure at 298 K was nearly the same for both concentrations, whereas at 10 bar, the selectivity was about 100 for 10% and 300 for 5%. Thus, as discussed in ref 5, the selectivity at 298 K was higher at lower pressures. In contrast to this, at 374 K, the selectivity increased with the pressure and with the concentration of NO_x in the ternary mixture. However, as expected, the selectivity was much lower at 374 K than at 298 K.

Additional test simulations of a fictitious system without the reaction showed that the high selectivity at 298 K and low pressure is a result of the selective adsorption while it is reduced somewhat by the presence of the chemical reaction.

In the adsorbed phase at 298 K, NO_x exist mainly as N₂O₄ and the flat N₂O₄ molecules are mainly situated close to the walls of the CNT. Their preferred orientation is parallel to the wall.

Additional MD simulations showed that all three molecule types can move in the z -direction within the narrow CNT (9,9). This was not trivial because of the size of the N₂O₄ molecule and the small tube diameter. The mobility of N₂ is necessary for ergodicity. Without such a mobility, the adsorption equilibrium that is established in the GEMC

simulation together with the RxMC simulation would not be reached in reality.

Simulation Methods. The method of GEMC simulations is a special Monte Carlo simulation method that combines two simulations in one. The method is described in the paper of Panagiotopoulos et al.⁴¹ and in many overview papers.^{42–44} In this method, here applied on CNTs, two simulation boxes are considered (box A for the gas phase mixture and box B for the adsorbed gas molecules within the CNT) that are in equilibrium with each other. In each box, shifts according to the Metropolis Monte Carlo algorithm take place. Additionally, always after the given time intervals, particles are transferred between the two boxes, in agreement with the principle of detailed balance, following the algorithm proposed by Rull et al.⁴⁵ The total number of molecules remains constant in usual GEMC simulations, i.e., when additional processes, like a chemical reaction, are not included, or when the concentration ratio in the gas box is not kept constant at a given value. The GEMC simulation has been used for the investigation of the adsorption of gases on porous materials by a homemade software, named Gibbon. This software, developed in 2011–2021, was used in Chokbunpiam et al.⁴ to examine the selective adsorption of nitrogen dioxide from the gas mixture with nitrogen in several ZIF materials. In Chanajaree et al.,¹⁷ the same software was used to investigate the separation of CO₂ and CH₄ from air on zeolitic imidazolate Framework-78. The software was used to fit a forcefield for the investigation of diffusion of hydrogen in ZIF-11 from experimental adsorption data by Schierz et al.⁴⁶ The diffusion was examined by MD simulations with other software. MD simulations of diffusion of a H₂/CH₄ gas mixture and investigation of structural changes by the adsorbed gases in ZIF-90 are investigated in Chokbunpiam et al.⁴⁷ and to calculate the membrane selectivity also, the adsorption selectivity was calculated using Gibbon. The same combination of MD for diffusion and Gibbon for adsorption of carbon in the MIL-127(Fe) MOF was used in Pongsajanukul et al.⁴⁸ The mixture CO₂/CO in MIL-127 has been studied in Chokbunpiam et al.⁴⁹ with the same methods.

In many papers that deal with the adsorption in porous solids, the GCMC simulations are used.^{15,31} Using the GCMC simulations, the chemical potentials of the adsorbed molecules must be known. This is not necessary for the GEMC simulation since the equilibrium between gas phase and adsorbed phase is simulated directly. The GEMC simulation also does not require knowledge of the pressure. This simulation method is entirely based on particle numbers and interactions. Since the volume of the gas box is known, we have the temperature and m densities characterizing the gas mixture of m particle sorts within the gas box. Thus, Gibbs rule is fulfilled.

In contrast to that, in laboratory experiments, particle densities, although also available, are rarely used for describing the system. Instead of particle densities, usually the pressure is used. Therefore, after the simulations, we calculated the pressure in the gas phase by the Peng–Robinson equation⁵⁰ for comparison of the results with the experiments. It was difficult to find the parameters of NO_x that are needed for the Peng–Robinson equation, because under ambient conditions, NO₂ and N₂O₄ exist only in coexistence and under the permanent chemical reaction (reaction 1) (see ref 3).

In the present paper, the adsorption equilibrium is simulated in conjunction with the equilibrium of the chemical reaction

(reaction 1). This reaction is simulated by the RxMC simulation within each box. The RxMC simulation is a special version of Monte Carlo simulations that can investigate chemical equilibria by analyzing the grand partition function of the mixture to find the most probable concentrations in the mixture. This method was developed in 1994 by two groups independently.^{51,52} After 1994, the RxMC simulation has been used in many applications. An overview of over applications until 2008 together with explanations of the method is given in ref 53. These applications include also chemical reactions within restricted geometries.^{37,38,54} More recent applications of the RxMC simulation for reactions in restricted geometries are given in refs 37, 38, and 55.

Good descriptions of the GEMC, GCMC, and RxMC simulations can be found within the review papers.^{43,44} The use of the GEMC and RxMC simulations for simulating the adsorption and reaction of the ternary mixture $N_2O_4/NO_2/N_2$ on a porous material (MIL-127) is described in the Supporting Information of ref 5. The paper⁵ and its Supporting Information can be downloaded for free from the homepage of the journal.

MD simulations are performed by using the DL-POLY program.⁵⁶ CNT and guest molecules have been considered to be rigid. One aim of these MD simulations is to prove that N_2 molecules still can escape from the CNT after some N_2O_4 have been adsorbed. If this would not be the case, then the high selectivity found in the GEMC simulations could not be reached in reality. The GEMC and the RxMC simulations are based on the assumption of ergodicity. This means reaching the adsorption equilibrium must not be blocked. The particle numbers used in MD are the same that were found in the GEMC simulations for the equilibrium.

The chemical reaction is neglected in these MD simulations because the GEMC simulation in connection with the RxMC simulation shows that almost only N_2O_4 molecules are found within the CNT for the conditions examined in these MD simulations.

AUTHOR INFORMATION

Corresponding Author

Supot Hannongbua – Computational Chemistry Unit Cell (CCUC), Department of Chemistry, Faculty of Science, Chulalongkorn University, Bangkok 10330, Thailand; Email: supot.h@chula.ac.th

Authors

Somphob Thompho – Pharmaceutical Research Instrument Center, Faculty of Pharmaceutical Sciences, Chulalongkorn University, Pathum Wan, Bangkok 10330, Thailand; orcid.org/0000-0002-3783-5883

Siegfried Fritzsche – Institute of Theoretical Physics, Leipzig University, 04081 Leipzig, Germany

Tatiya Chokbunpiam – Department of Chemistry and Center of Excellence for Innovation in Chemistry Faculty of Science, Ramkhamhaeng University, Bangkok 10240, Thailand; orcid.org/0000-0002-7679-376X

Tawun Remsungnen – Faculty of Interdisciplinary Studies, Khon Kaen University, Nong Khai 43000, Thailand; orcid.org/0000-0001-7169-4482

Wolfhard Janke – Institute of Theoretical Physics, Faculty of Physics and Geosciences, Leipzig University, 04081 Leipzig, Germany; orcid.org/0000-0002-5165-9097

Complete contact information is available at:

<https://pubs.acs.org/10.1021/acsomega.1c01459>

Notes

The authors declare no competing financial interest.

ACKNOWLEDGMENTS

We acknowledge financial support from the Grants for Development of New Faculty Staff, Ratchadaphiseksomphot Endowment Fund. Thailand's National e-Science Infrastructure Consortium is acknowledged for computer resources. S.F. and T.R. thank the Khon Kaen University for International Visiting Scholar 2019. We also thank the computer center of the University of Leipzig for computing resources and Mr. Rost for kind support. T.C. and T.R. would like to thank the Malaysia-Thailand Joint Authority (MTJA) Research Cess Fund (RCF) and the Center of Excellence for Innovation in Chemistry (PERCH-CIC), Office of the Higher Education Commission, Ministry of Education (OHEC) Research, for computer time and facilities. T.C. and S.H. would like to thank the Ministry of High Education, Science, Research and Innovation (RGNS 63-210) for support.

REFERENCES

- (1) Chen, T.-M.; Kuschner, W. G.; Gokhale, J.; Shofer, S. Outdoor Air Pollution: Nitrogen Dioxide, Sulfur Dioxide, and Carbon Monoxide Health Effects. *Am. J. Med. Sci.* **2007**, *333*, 249–256.
- (2) Seddiq, I. S.; Elgohary, M. M. Eco-friendly selection of ship emissions reduction strategies with emphasis on SO_x and NO_x emissions. *Int. J. Nav. Archit. Ocean Eng.* **2014**, *6*, 737–748.
- (3) Chao, J.; Wilhoit, R. C.; Zwolinski, B. J. Gas phase chemical equilibrium in dinitrogen trioxide and dinitrogen tetroxide. *Thermochim. Acta* **1974**, *10*, 359–371.
- (4) Chokbunpiam, T.; Chanajaree, R.; Caro, J.; Janke, W.; Remsungnen, T.; Hannongbua, S.; Fritzsche, S. Separation of nitrogen dioxide from the gas mixture with nitrogen by use of ZIF materials; computer simulation studies. *Comput. Mater. Sci.* **2019**, *168*, 246–252.
- (5) Fritzsche, S.; Chokbunpiam, T.; Caro, J.; Hannongbua, S.; Janke, W.; Remsungnen, T. Combined Adsorption and Reaction in the Ternary Mixture N_2 , N_2O_4 , NO_2 on MIL-127 Examined by Computer Simulations. *ACS Omega* **2020**, *5*, 13023–13033.
- (6) Li, J.; Han, X.; Zhang, X.; Sheveleva, A. M.; Cheng, Y.; Tuna, F.; McInnes, E. J. L.; McCormick McPherson, L. J.; Teat, S. J.; Daemen, L. L.; Ramirez-Cuesta, A. J.; Schröder, M.; Yang, S. Capture of nitrogen dioxide and conversion to nitric acid in a porous metal-organic framework. *Nat. Chem.* **2019**, *11*, 1085–1090.
- (7) Lévassieur, B.; Petit, C.; Bandoz, T. J. Reactive Adsorption of NO_2 on Copper-Based Metal–Organic Framework and Graphite Oxide/Metal–Organic Framework Composites. *ACS Appl. Mater. Interfaces* **2010**, *2*, 3606–3613.
- (8) Ebrahim, A. M.; Bandoz, T. J. Ce(III) Doped Zr-Based MOFs as Excellent NO_2 Adsorbents at Ambient Conditions. *ACS Appl. Mater. Interfaces* **2013**, *5*, 10565–10573.
- (9) Petit, C.; Bandoz, T. J. Exploring the coordination chemistry of MOF–graphite oxide composites and their applications as adsorbents. *Dalton Trans.* **2012**, *41*, 4027–4035.
- (10) Han, X.; Godfrey, H. G. W.; Briggs, L.; Davies, A. J.; Cheng, Y.; Daemen, L. L.; Sheveleva, A. M.; Tuna, F.; McInnes, E. J. L.; Sun, J.; Drathen, C.; George, M. W.; Ramirez-Cuesta, A. J.; Thomas, K. M.; Yang, S.; Schröder, M. Reversible adsorption of nitrogen dioxide within a robust porous metal–organic framework. *Nat. Mater.* **2018**, *17*, 691–696.
- (11) Tan, K.; Zuluaga, S.; Gong, Q.; Gao, Y.; Nijem, N.; Li, J.; Thonhauser, T.; Chabal, Y. J. Competitive Coadsorption of CO_2 with H_2O , NH_3 , SO_2 , NO , NO_2 , N_2 , O_2 , and CH_4 in M-MOF-74 (M = Mg, Co, Ni): The Role of Hydrogen Bonding. *Chem. Mater.* **2015**, *27*, 2203–2217.

- (12) Rubel, A. M.; Stencel, J. M. Effect of Pressure on NO_x Adsorption by Activated Carbons. *Energy Fuels* **1996**, *10*, 704–708.
- (13) Fioretos, K. A.; Psfogiannakis, G. M.; Froudakis, G. E. Ab-Initio Study of the Adsorption and Separation of NO_x and SO_x Gases in Functionalized IRMOF Ligands. *J. Phys. Chem. C* **2011**, *115*, 24906–24914.
- (14) Sun, W.; Lin, L.-C.; Peng, X.; Smit, B. Computational screening of porous metal-organic frameworks and zeolites for the removal of SO₂ and NO_x from flue gases. *AIChE J.* **2014**, *60*, 2314–2323.
- (15) Matito-Martos, I.; Rahbari, A.; Martin-Calvo, A.; Dubbeldam, D.; Vlugt, T. J. H.; Calero, S. Adsorption equilibrium of nitrogen dioxide in porous materials. *Phys. Chem. Chem. Phys.* **2018**, *20*, 4189–4199.
- (16) Myers, A. L. Thermodynamics of Adsorption. In *Chemical Thermodynamics for Industry*; Letcher, T., Ed.; The Royal Society of Chemistry, 2004; pp 243–253.
- (17) Chanajaree, R.; Chokbunpiam, T.; Kärger, J.; Hannongbua, S.; Fritzsche, S. Investigating adsorption- and diffusion selectivity of CO₂ and CH₄ from air on zeolitic imidazolate Framework-78 using molecular simulations. *Microporous Mesoporous Mater.* **2019**, *274*, 266–276.
- (18) Kowalczyk, P. Molecular insight into the high selectivity of double-walled carbon nanotubes. *Phys. Chem. Chem. Phys.* **2012**, *14*, 2784–2790.
- (19) Iijima, S.; Ichihashi, T. Single-shell carbon nanotubes of 1-nm diameter. *Nature* **1993**, *363*, 603–605.
- (20) Bethune, D. S.; Kiang, C. H.; De Vries, M. S.; Gorman, G.; Savoy, R.; Vazquez, J.; Beyers, R. Cobalt-catalysed growth of carbon nanotubes with single-atomic-layer walls. *Nature* **1993**, *363*, 605–607.
- (21) Ajayan, P. M.; Lijima, S. Smallest carbon nanotube. *Nature* **1992**, *358*, 23–23.
- (22) De Volder, M. F. L.; Tawfick, S. H.; Baughman, R. H.; Hart, A. J. Carbon Nanotubes: Present and Future Commercial Applications. *Science* **2013**, *339*, 535.
- (23) Niyogi, S.; Hamon, M. A.; Hu, H.; Zhao, B.; Bhowmik, P.; Sen, R.; Itkis, M. E.; Haddon, R. C. Chemistry of Single-Walled Carbon Nanotubes. *Acc. Chem. Res.* **2002**, *35*, 1105–1113.
- (24) Feng, S.; Li, X.; Zhao, S.; Hu, Y.; Zhong, Z.; Xing, W.; Wang, H. Multifunctional metal organic framework and carbon nanotube-modified filter for combined ultrafine dust capture and SO₂ dynamic adsorption. *Environ. Sci.: Nano* **2018**, *5*, 3023–3031.
- (25) Pandey, S. K.; Vishwakarma, P. K.; Yadav, S. K.; Shukla, P.; Srivastava, A. Multiwalled Carbon Nanotube Filters for Toxin Removal from Cigarette Smoke. *ACS Appl. Nano Mater.* **2020**, *3*, 760–771.
- (26) Frey, J. T.; Doren, D. J. TubeGen 3.4, Web-Accessible Nanotube Structure Generator. <https://turin.nss.udel.edu/research/tubegenonline.html>.
- (27) Avogadro. Chemistry-Free Cross Platform Molecular Editor. <https://Avogadro.cc>.
- (28) *Materials Studio*; Accelrys Software, Inc.: San Diego, 2007.
- (29) Pfrommer, B. G.; Cote, M.; Louie, S. G.; Cohen, M. L. Relaxation of crystals with the quasi-Newton method. *J. Comput. Phys.* **1997**, *131*, 233–240.
- (30) Milman, V.; Winkler, B.; White, J. A.; Pickard, C. J.; Payne, M. C.; Akhmatkaya, E. V.; Nobes, R. H. Electronic structure, properties, and phase stability of inorganic crystals: A pseudopotential plane-wave study. *Int. J. Quantum Chem.* **2000**, *77*, 895–910.
- (31) Zhang, H.; Zeng, X.; Zhao, Z.; Zhai, Z.; Cao, D. Adsorption and selectivity of CH₄/CO₂ in functional group rich organic shales. *J. Nat. Gas Sci. Eng.* **2017**, *39*, 82–89.
- (32) Pramanik, C.; Gissinger, J. R.; Kumar, S.; Heinz, H. Carbon Nanotube Dispersion in Solvents and Polymer Solutions: Mechanisms, Assembly, and Preferences. *ACS Nano* **2017**, *11*, 12805–12816.
- (33) Kaukonen, M.; Gulans, A.; Havu, P.; Kauppinen, E. Lennard-Jones parameters for small diameter carbon nanotubes and water for molecular mechanics simulations from van der Waals density functional calculations. *J. Comput. Chem.* **2012**, *33*, 652–658.
- (34) Bourasseau, E.; Lachet, V.; Desbiens, N.; Maillet, J. B.; Teuler, J. M.; Ungerer, P. Thermodynamic Behavior of the CO₂ + NO₂/N₂O₄ Mixture: A Monte Carlo Simulation Study. *J. Phys. Chem. B* **2008**, *112*, 15783–15792.
- (35) Potoff, J. J.; Siepmann, J. I. Vapor-liquid equilibria of mixtures containing alkanes, carbon dioxide, and nitrogen. *AIChE J.* **2001**, *47*, 1676–1682.
- (36) Roscoe, H. K.; Hind, A. K. The equilibrium constant of NO₂ with N₂O₄ and the temperature dependence of the visible spectrum of NO₂: A critical review and the implications for measurements of NO₂ in the polar stratosphere. *J. Atmos. Chem.* **1993**, *16*, 257–276.
- (37) Borówko, M.; Patrykiewicz, A.; Sokółowski, S.; Zagórski, R.; Pizio, O. Chemical reactions at surfaces: Application of the reaction ensemble Monte Carlo method. *Czech. J. Phys.* **1998**, *48*, 371–388.
- (38) Borówko, M.; Zagórski, R. Chemical equilibria in slitlike pores. *J. Chem. Phys.* **2001**, *114*, 5397–5403.
- (39) Stai, D. F.; Bizjak, F.; Stephanou, S. E. Thermodynamic properties of nitrogen tetroxide. *J. Spacecr. Rockets* **1965**, *2*, 742–745.
- (40) Kärger, J. *Diffusion under Confinement*; Sachsische Akademie der Wissenschaften zu Leipzig: Lipsia, 2003.
- (41) Panagiotopoulos, A. Z.; Quirke, N.; Stapleton, M.; Tildesley, D. J. Phase equilibria by simulation in the Gibbs ensemble. *Mol. Phys.* **1988**, *63*, 527–545.
- (42) Frenkel, D.; Smit, B., Eds. *Understanding Molecular Simulation*, 2nd ed.; Academic Press: San Diego, 2002; pp 201–225.
- (43) Theodorou, D. N. Progress and Outlook in Monte Carlo Simulations. *Ind. Eng. Chem. Res.* **2010**, *49*, 3047–3058.
- (44) Dubbeldam, D.; Torres-Knoop, A.; Walton, K. S. On the inner workings of Monte Carlo codes. *Mol. Simul.* **2013**, *39*, 1253–1292.
- (45) Rull, L. F.; Jackson, G.; Smit, B. The Condition of Microscopic Reversibility in Gibbs Ensemble Monte-Carlo Simulations of Phase-Equilibria. *Mol. Phys.* **1995**, *85*, 435–447.
- (46) Schierz, P.; Fritzsche, S.; Janke, W.; Hannongbua, S.; Saengsawang, O.; Chmelik, C.; Kärger, J. MD simulations of hydrogen diffusion in ZIF-11 with a force field fitted to experimental adsorption data. *Microporous Mesoporous Mater.* **2015**, *203*, 132–138.
- (47) Chokbunpiam, T.; Fritzsche, S.; Caro, J.; Chmelik, C.; Janke, W.; Hannongbua, S. Importance of ZIF-90 Lattice Flexibility on Diffusion, Permeation, and Lattice Structure for an adsorbed H₂/CH₄ Gas Mixture: A Re-Examination by Gibbs Ensemble Monte Carlo and Molecular Dynamics Simulations. *J. Phys. Chem. C* **2017**, *121*, 10455–10462.
- (48) Pongsajanukul, P.; Parasuk, V.; Fritzsche, S.; Assabumrungrat, S.; Wongsakulphasatch, S.; Bovornratanaraks, T.; Chokbunpiam, T. Theoretical study of carbon dioxide adsorption and diffusion in MIL-127(Fe) metal organic framework. *Chem. Phys.* **2017**, *491*, 118–125.
- (49) Chokbunpiam, T.; Fritzsche, S.; Parasuk, V.; Caro, J.; Assabumrungrat, S. Molecular simulations of a CO₂/CO mixture in MIL-127. *Chem. Phys. Lett.* **2018**, *696*, 86–91.
- (50) Peng, D.-Y.; Robinson, D. B. A New Two-Constant Equation of State. *Ind. Eng. Chem. Fundam.* **1976**, *15*, 59–64.
- (51) Smith, W. R.; Triska, B. The reaction ensemble method for the computer simulation of chemical and phase equilibria. I. Theory and basic examples. *J. Chem. Phys.* **1994**, *100*, 3019–3027.
- (52) Johnson, J. K.; Panagiotopoulos, A. Z.; Gubbins, K. E. Reactive canonical Monte Carlo. *Mol. Phys.* **1994**, *81*, 717–733.
- (53) Heath Turner, C.; Brennan, J. K.; Lísál, M.; Smith, W. R.; Karl Johnson, J.; Gubbins, K. E. Simulation of chemical reaction equilibria by the reaction ensemble Monte Carlo method: A review. *Mol. Simul.* **2008**, *34*, 119–146.
- (54) Jakobtorweihen, S.; Hansen, N.; Keil, F. J. Combining reactive and configurational-bias Monte Carlo: Confinement influence on the propene metathesis reaction system in various zeolites. *J. Chem. Phys.* **2006**, *125*, No. 224709.
- (55) Furmaniak, S.; Gauden, P. A.; Kowalczyk, P.; Patrykiewicz, A. Monte Carlo study of chemical reaction equilibria in pores of activated carbons. *RSC Adv.* **2017**, *7*, 53667–53679.
- (56) Smith, W.; Todorov, I. T. A short description of DL_POLY. *Mol. Simul.* **2006**, *32*, 935–943.